Title

Peripheral-derived regulatory T cells contribute to tumor-mediated immune suppression in a nonredundant manner.

Journal

Proceedings of the National Academy of Sciences of the United States of America, 121(36)

Authors

Hossain, Md

King, Paul

Hackett, Justin

et al.

Publication Date

2024-09-03

DOI

10.1073/pnas.2404916121

Peer reviewed

PNAS RESEARCH ARTICLE | IMMUNOLOGY AND INFLAMMATION

Peripheral-derived regulatory T cells contribute to tumor-mediated immune suppression in a nonredundant manner

Md Moazzem Hossain[a], Paul King[a], Justin Hackett[b], Herve C. Gerard[a], Rajmund Niwinski[a], Lan Wu[c], Luc Van Kaer[c], Gregory Dyson[b,d], Heather Gibson[a,b,d], Alexander D. Borowsky[e], and Eric Sebzda[a,d,1]

Affiliations are included on p. 10.

Edited by Gordon Freeman, Dana-Farber Cancer Institute, Boston, MA; received March 8, 2024; accepted July 30, 2024

Identifying tumor-mediated mechanisms that impair immunity is instrumental for the design of new cancer therapies. Regulatory T cells (Tregs) are a key component of cancer-derived immune suppression; however, these lymphocytes are necessary to prevent systemic autoimmunity in mice and humans, and thus, direct targeting of Tregs is not a clinical option for cancer patients. We have previously demonstrated that excising transcription factor Kruppel-like factor 2 (*Klf2*) within the T cell lineage blocks the generation of peripheral-derived Tregs (pTregs) without impairing production of thymic-derived Tregs. Using this mouse model, we have now demonstrated that eliminating pTregs is sufficient to delay/prevent tumor malignancy without causing autoimmunity. Cancer-bearing mice that expressed KLF2 converted tumor-specific CD4$^+$ T cells into pTregs, which accumulated in secondary lymphoid organs and impaired further T cell effector activity. In contrast, pTreg-deficient mice retained cancer-specific immunity, including improved T cell infiltration into "cold" tumors, reduced T cell exhaustion in tumor beds, restricted generation of tumor-associated myeloid-derived suppressor cells, and the continued production of circulating effector T cells that arose in a cancer-dependent manner. Results indicate that tumor-specific pTregs are critical for early stages of cancer progression and blocking the generation of these inhibitory lymphocytes safely delays/prevents malignancy in preclinical models of melanoma and prostate cancer.

regulatory T cells | prostate cancer | melanoma | pTregs | KLF2

Significance

Cancers suppress host immunity to achieve malignancy, and regulatory T cells (Tregs) play a crucial role in this process. However, Tregs also prevent lethal autoimmunity, and thus, direct targeting of Tregs is not a viable cancer therapy at present. We now show that a subset of Tregs, termed peripheral Tregs (pTregs), are necessary for melanoma and prostate cancer progression, and mice that lack pTregs can avoid malignancy. Importantly, elimination of pTregs does not lead to overt pathology associated with autoimmunity. Instead, blocking the generation of pTregs in preclinical mouse models improved immune responses that correlate with positive cancer patient outcomes. This study indicates that pTregs are a viable target to safely enhance anticancer immunity.

Numerous immune regulatory mechanisms maintain self-tolerance, and tumors co-opt these events to avoid immune detection and blunt immune-based cancer therapies. For example, Foxp3$^+$ regulatory T cells (Tregs) are a subset of CD4$^+$ T lymphocytes that are necessary to prevent lethal autoimmunity (1–3); however, elimination of Tregs improves antitumor immunity (4–9), demonstrating that cancers use Tregs to escape tumor surveillance. Tregs are composed of at least two lineages: thymic-derived Tregs (tTregs) that originate from self-reactive thymocytes during T cell development (10) and peripheral-derived Tregs (pTregs) that arise from naive CD4$^+$ T cells that are activated in the presence of tolerizing cytokines (11). [Note: tTregs and pTregs are sometimes referred to as "natural" and "induced" Tregs, respectively; however, we will use the nomenclature recommended at the Third International Conference on Tregs (12)]. Treg-mediated suppression is initially directed by T cell receptor specificity (13–15), which suggests that a primary difference between Treg lineages is a bias toward endogenous (tTregs) versus exogenous (pTregs) antigens. Most tumors can initiate an immune response in mice and humans (16), arguing that exogenous antigens (neoantigens) are commonly associated with cancers. If true, then eliminating pTregs while retaining tTregs could theoretically prevent cancers from avoiding antitumor immune responses while maintaining self-tolerance. Using genetically modified mice that lack pTregs but retain tTregs, we found that such animals were resistant to transplanted and spontaneous forms of cancer but did not develop autoimmune pathologies. These results indicate that temporarily blocking pTreg development is a safe means of delaying/preventing cancer and may complement immunotherapies that reengage antitumor T cell activity.

Results

A Kruppel-Like Factor 2 (KLF2)-Dependent T Cell Event Promotes Tumor Malignancy. The transcription factor, *KLF2*, is critical for the transition of CD4$^+$ T cells into pTregs but is not required for tTreg development or Treg-mediated immune suppression (17) (Fig. 1*A*). Therefore, T cell–specific excision of *Klf2* using a Cre-Lox mouse model (Lck-cre; Klf2$^{fl/fl}$) allowed us to investigate the potential role of pTregs in cancer progression

Author contributions: M.H., H.C.G., and E.S. designed research; M.H., P.K., J.H., H.C.G., R.N., L.W., H.G., A.D.B., and E.S. performed research; L.V.K., G.D., A.D.B., and E.S. analyzed data; and L.V.K., G.D., A.D.B., and E.S. wrote the paper.

The authors declare no competing interest.

This article is a PNAS Direct Submission.

[1]To whom correspondence may be addressed. Email: eric.sebzda@wayne.edu.

This article contains supporting information online at https://www.pnas.org/lookup/suppl/doi:10.1073/pnas.2404916121/-/DCSupplemental.

Published August 29, 2024.

and antitumor immunity. To initially test whether tumor-specific T cell responses were influenced by pTregs, Lck-cre; Klf2$^{fl/fl}$ mice and littermate controls were intravenously challenged with a B16 melanoma cell line. Two weeks postchallenge, T cells from control mice no longer proliferated in response to tumor antigens (Fig. 1*B*). In contrast, antitumor T cell responses were retained in animals that lacked pTregs. Expanding on this study, tumor growth (Fig. 1*C*) and survival curves (Fig. 1*D*) were established following the subcutaneous (s.c.) transplantation of B16 melanoma. Again, antitumor immune responses were

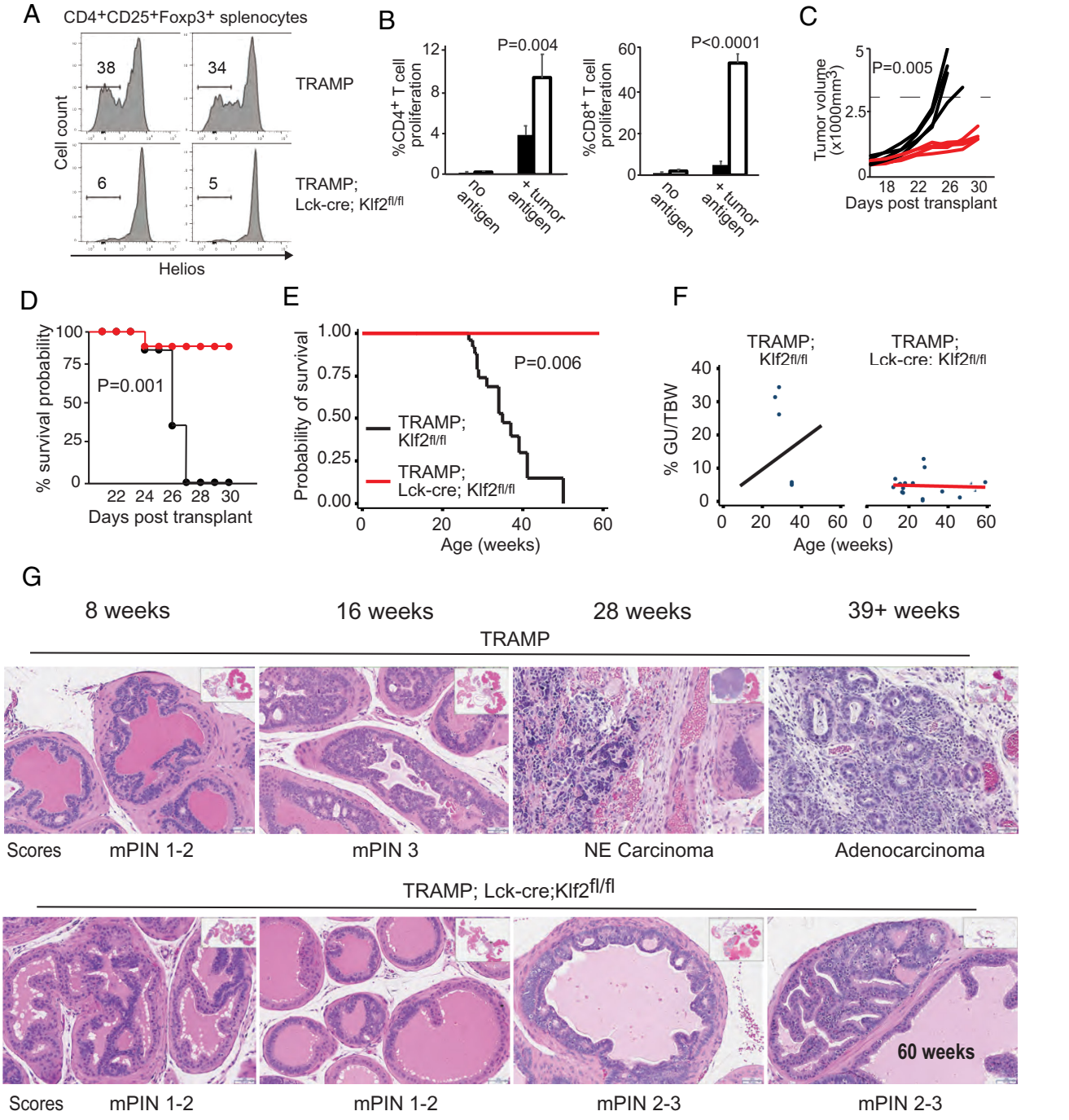

Fig. 1. Excision of *Klf2* within the T cell compartment impedes malignant cancer. (*A*) Tregs harvested from Lck-cre; Klf2$^{fl/fl}$ mice express high levels of transcription factor Helios, which is consistent with these cells being confined to the tTreg lineage. The percentage of Helios^{low} pTregs is shown in each histogram. N = 2 mice per cohort. (*B*) T cell proliferation in response to B16 antigen. Lck-cre; Klf2$^{fl/fl}$ (white bars) and Klf2$^{fl/fl}$ (black bars) littermates were challenged i.v. with B16 melanoma; then, splenocytes were restimulated ex vivo with B16 lysate to elicit tumor-specific activity. Proliferation (CFSE dilution, cultured in triplicate) was measured by flow cytometry. *P* values (Student's *t* test) and error bars (SD) are shown. N = 2 experiments. (*C*) B16 tumor progression in Lck-cre; Klf2$^{fl/fl}$ mice. Four Klf2$^{fl/fl}$ (black) and Lck-cre; Klf2$^{fl/fl}$ (red) littermates were challenged s.c. with B16 melanoma (10^4), and tumor volume was measured over time. *P* = 0.005, calculated using the Wilcoxon signed rank-sum test at 26 d posttransplant. N = 2 experiments. (*D*) Survival estimates of mice challenged s.c. with B16 melanoma. Kaplan–Meier curves using 8 Klf2$^{fl/fl}$ (black) and 10 Lck-cre; Klf2$^{fl/fl}$ (red) mice. *P* = 0.001, calculated using a log-rank test. (*E*) Survival estimates for TRAMP versus TRAMP; Lck-cre; Klf2$^{fl/fl}$ littermates. A Kaplan–Meier survival curve was generated with 45 TRAMP (black line) and 28 TRAMP; Lck-cre; Klf2$^{fl/fl}$ (red line) mice. *P* = 0.006, calculated using a log-rank test. (*F*) PCa progression in TRAMP cohorts. The % genitourinary tract weight (GU) relative to TBW was plotted over time. Lines are fitted values. *P* = 0.008; the *P*-value tests the difference of slope between the two TRAMP cohorts via an interaction term in a linear regression model. (*G*) Histological analysis of prostates harvested from TRAMP (*Top*) versus TRAMP; Lck-cre; Klf2$^{fl/fl}$ (*Bottom*) mice at indicated time points. H&E, 20× magnification. Pathologic scores are assigned to each tissue.

significantly improved in Lck-cre; Klf2$^{fl/fl}$ mice relative to control littermates, which suggested that pTregs contributed to cancer progression. B16 melanoma is an aggressive cancer that quickly establishes an immune-suppressive microenvironment. Although this is advantageous for short-term studies, it raised concerns about physiological relevance. To address this issue, we selected an autochthonous cancer model (Transgenic Adenocarcinoma Mouse Prostate, TRAMP) to investigate how *Klf2* excision within the T cell compartment impacted spontaneous prostate cancer (PCa) progression. This model has previously been used to validate cancer immunotherapies (18–22), thus demonstrating its use in testing antitumor immunity. TRAMP mice express SV40 T antigen (TAg) under the prostate-specific promoter, probasin, which drives PCa development in postpubescent male mice (23). TRAMP mice develop prostatic intraepithelial neoplasia (PIN), a premalignant lesion that closely mirrors early stages of human PCa. PIN then progresses to neuroendocrine PCa, a metastatic tumor stage that emerges in PCa patients who no longer respond to hormonal treatment. In keeping with published results (24), control TRAMP animals had a mean survival time of 40 ± 5 wk and all TRAMP mice succumbed to malignancy by 60 wk of age (Fig. 1*E*). In contrast, none of the TRAMP; Lck-cre; Klf2$^{fl/fl}$ mice reached a humane end point that required killing. Cancerous prostate mass increases relative to total body weight (TBW) in TRAMP animals, so the ratio of genitourinary tract (GU) to TBW was used to quantify PCa progression. TRAMP mice tripled their GU:TBW ratio over a 50-wk time period, whereas the GU:TBW ratio remained constant in TRAMP; Lck-cre; Klf2$^{fl/fl}$ littermates (GU:TBW shown in Fig. 1*F*, GU weight shown in *SI Appendix*, Fig. S1). To confirm that PCa progression was halted in TRAMP; Lck-cre; Klf2$^{fl/fl}$ mice, prostate histopathology was scored at set time points reflecting general occurrence of PIN (8 to 16 wk) and NEPCa (24+ wk) in TRAMP animals. Early stages of PIN could be observed in TRAMP; Lck-cre; Klf2$^{fl/fl}$ mice, demonstrating that *Klf2* excision did not impact epithelial cell transformation (Fig. 1*G*). Conversely, neither late-stage PIN nor NEPCa was present in TRAMP; Lck-cre; Klf2$^{fl/fl}$ animals. Therefore, we conclude that cancers, including an autochthonous model of PCa, require a KLF2-dependent T cell event to avoid immune detection and progress toward malignancy.

pTregs Are Necessary for Cancer Progression. Of the reported mouse models that impact pTreg ontogeny (17, 25–28), *Klf2* gene-targeted animals possess the most stringent phenotype in terms of pTreg blockade, and thus, these animals were relied upon in the present study. To prevent pTreg differentiation, *Klf2* had to be excised prior to Foxp3 expression in CD4$^+$ T cells. This meant that in addition to lacking pTregs, (TRAMP); Lck-cre; Klf2$^{fl/fl}$ mice harbored KLF2-deficient tTregs and T cells. These animals were viable and did not suffer from systemic autoimmunity, which suggested that KLF2-deficient tTregs were functional; however, there was the formal possibility that a KLF2-dependent tTreg function was lacking in these mice and this was the underlying cause of tumor resistance. To test this possibility, TRAMP; Foxp3-cre; Klf2$^{fl/fl}$ mice were generated. Although KLF2 is required for Foxp3 expression during CD4$^+$ T cell differentiation into a pTreg, KLF2 is not required for Foxp3 activity once this latter transcription factor is expressed. For this reason, Foxp3-cre; Klf2$^{fl/fl}$ mice generate both KLF2-deficient tTregs and pTregs (17). As previously reported (29), these animals also exhibited spontaneous autoimmune phenotypes. Antitumor immunity often corresponds with autoimmunity due to impaired peripheral tolerance (30), yet TRAMP; Foxp3-cre; Klf2$^{fl/fl}$ mice continued to develop malignant PCa (Fig. 2 *A* and *B*). Therefore, we conclude that defective suppression by KLF2-deficient tTregs was not responsible for tumor resistance in (TRAMP); Lck-cre; Klf2$^{fl/fl}$ animals.

An alternative explanation for cancer resistance in (TRAMP); Lck-cre; Klf2$^{fl/fl}$ animals was a tumor-specific gain-of-function within the KLF2-deficient T cell compartment. For instance, KLF2-deficient T cells are biased to leave secondary lymphoid organs (SLOs) and enter peripheral tissues (31). Clinical studies have shown a correlation between tumor-infiltrating lymphocyte (TIL) frequencies and cancer outcomes, and therefore, it was possible that altered T cell migration patterns were responsible for improved antitumor immunity in (TRAMP); Lck-cre; Klf2$^{fl/fl}$ mice. As well, KLF2-deficient CD4$^+$ T cells can preferentially skew toward a T_{FH} cell lineage (32, 33); a population that contributes to antitumor immunity in cancer models (34–37). Therefore, to test for potential gain-of-function phenotypes, mixed bone marrow chimeric TRAMP animals were generated. Briefly, lethally irradiated TRAMP; Lck-cre; Klf2$^{fl/fl}$ mice received a 5:1 ratio of T cell-depleted bone marrow from Lck-cre; Klf2$^{fl/fl}$ and Klf2$^{fl/fl}$ donors; then, the chimeric mice were killed 28 wk later to assess PCa progression (Fig. 2*C*). TRAMP; Lck-cre; Klf2$^{fl/fl}$ mice were selected as recipients to ensure that radiation-resistant Tregs did not impact this study (38–40). An increased proportion of Lck-cre; Klf2$^{fl/fl}$ bone marrow was used to compensate for reduced KLF2-deficient T cell migration to SLOs (29, 31) and to optimize our ability to observe potential gain-of-function phenotypes. Histopathology (Fig. 2*D*) and GU/TBW ratios demonstrated that the chimeric TRAMP animals developed malignant PCa akin to TRAMP mice, and in contrast to Lck-cre; Klf2$^{fl/fl}$ control animals. Consistent with a suppressive lineage being present in KLF2-replete cells, we similarly found that a chimeric Lck-cre; Klf2$^{fl/fl}$ mouse (5:1 ratio of Lck-cre; Klf2$^{fl/fl}$ to Klf2$^{fl/fl}$ bone marrow) challenged s.c. with TRAMP-C2 tumor succumbed to malignancy (*SI Appendix*, Fig. S2*A*). The TRAMP-C2 cell line is derived from a 32-wk-old TRAMP mouse; however, TRAMP-C2 no longer expresses SV40 TAg (41). Despite this fact, Lck-cre; Klf2$^{fl/fl}$ mice displayed improved antitumor immunity (*SI Appendix*, Fig. S2*B*), indicating that anti-PCa immunity was not limited to a single oncogenic antigen in these animals. To further demonstrate that cancer progression was contingent upon a suppressive T cell population found in wild-type animals, we adoptively transferred naive CD4$^+$ T cells into Lck-cre; Klf2$^{fl/fl}$ recipients that had been challenged with TRAMP-C2. As shown in Fig. 2*E*, KLF2$^+$ CD4$^+$ T cells alone were sufficient to interfere with anticancer immunity in Lck-cre; Klf2$^{fl/fl}$ mice. Interestingly, we were also able to observe the de novo generation of pTregs within the draining lymph node of tumor-bearing recipients (Fig. 2*F*). Based on this finding, we decided to directly test the causal role of pTregs in cancer progression by transferring tumor-specific pTregs into tumor-bearing Lck-cre; Klf2$^{fl/fl}$ animals (Fig. 2*G*). In this case, a B16 melanoma line that expresses chicken ovalbumin (OVA) was injected s.c. into Lck-cre; Klf2$^{fl/fl}$ mice; then, naive CD4$^+$ T cells from OT2; Foxp3^{RFP} animals (CD4$^+$ T cells express a TCR transgene specific for $OVA_{323-339}$+I-A^b; Tregs express monomeric red fluorescent protein) were adoptively transferred after tumor establishment. Ten days after the initial transfer of mRFP$^-$ CD4$^+$ T cells, we were able to isolate and transfer mRFP$^+$ pTregs into a new set of Lck-cre; Klf2$^{fl/fl}$ recipients that had established B16-OVA melanoma. Akin to wild-type mice, Lck-cre; Klf2$^{fl/fl}$ animals that received tumor-specific pTregs developed malignant cancer that required killing (Fig. 2*H*). This contrasted with pTreg-deficient Lck-cre; Klf2$^{fl/fl}$ mice that retained superior antitumor immunity. From this, we conclude that tumor-specific pTregs, derived from KLF2$^+$ CD4$^+$ T cells, were responsible for tumor progression in mixed lymphocyte studies (Figs. 2 *D* and *E*) and impaired pTreg

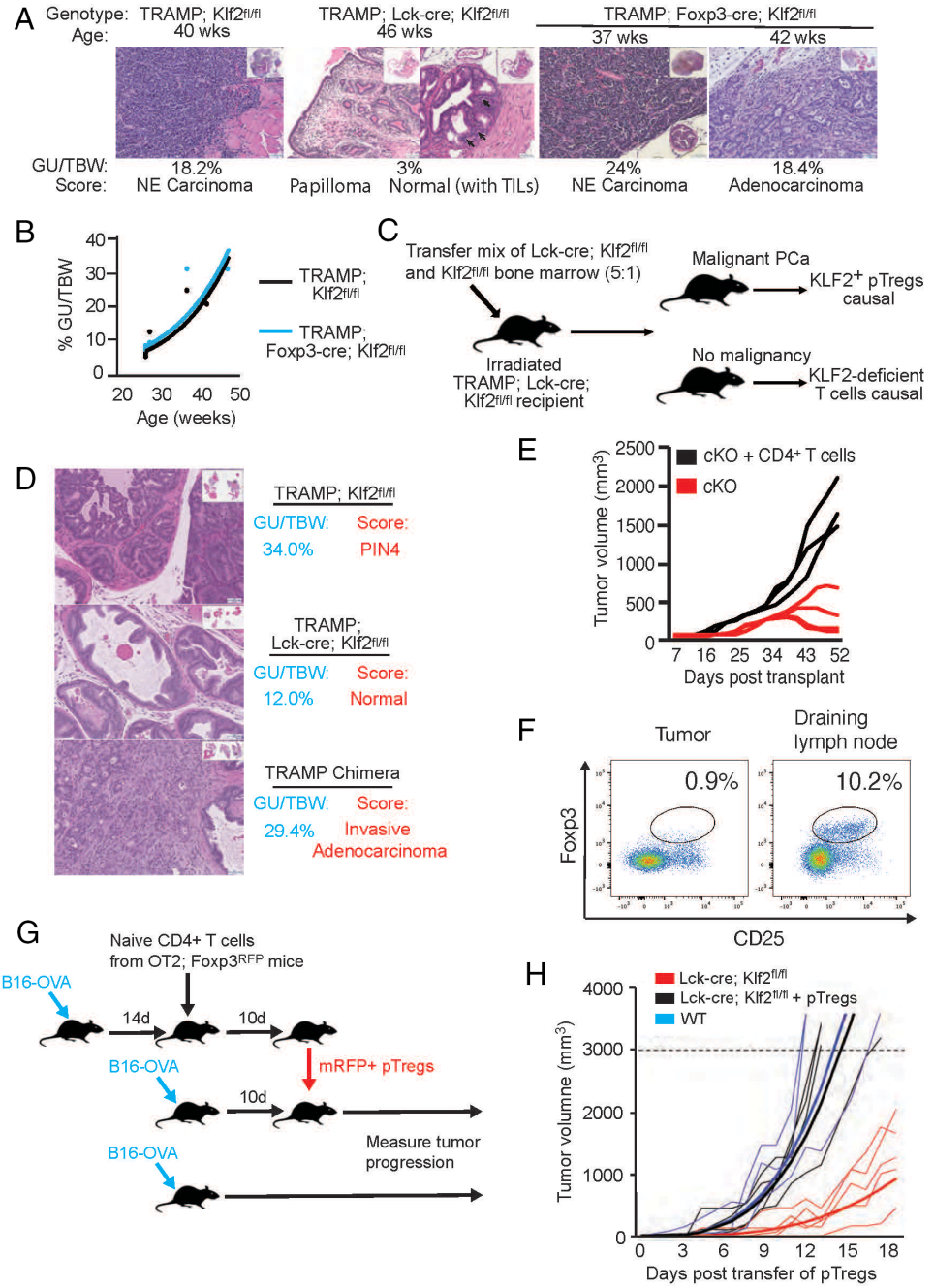

Fig. 2. pTregs are necessary and sufficient for PCa progression. (*A*) Histological analysis of prostates from control (TRAMP and TRAMP; Lck-cre; Klf2$^{fl/fl}$) versus TRAMP; Foxp3-cre; Klf2$^{fl/fl}$ mice. H&E, 10× magnification. The age of each animal, extent of tumor growth (GU relative to TBW), and pathology score assigned to each tissue are shown. Arrows in TRAMP; Lck-cre; Klf2$^{fl/fl}$ prostate (*Right*) indicate sites of TIL. (*B*) PCa progression in TRAMP; Foxp3-cre; Klf2$^{fl/fl}$ mice. Percent GU/TBM increase over time is shown for TRAMP (black) versus TRAMP; Foxp3-cre; Klf2$^{fl/fl}$ (blue) littermates. Nine mice per cohort. Linear regression identified no significant difference between the lines, $P > 0.05$. (*C*) Generation of mixed bone marrow chimeric animals. Lethally irradiated TRAMP; Lck-cre; Klf2$^{fl/fl}$ mice received a 5:1 ratio of Lck-cre; Klf2$^{fl/fl}$ and Klf2$^{fl/fl}$ bone marrow to generate animals that had both KLF2-deficient T cells and KLF2-replete pTregs. (*D*) PCa progression in a TRAMP; Lck-cre; Klf2$^{fl/fl}$ mixed bone marrow chimeric mouse. Prostate histology (H&E, 10× magnification), percent GU/TBW (blue font), and tissue pathology score (red font) are shown for a TRAMP (*Top*), TRAMP; Lck-cre; Klf2$^{fl/fl}$ (*Middle*), and a TRAMP; Lck-cre; Klf2$^{fl/fl}$ chimeric mouse (*Bottom*). Mice were 32 to 35 wk of age when they were killed. Three chimeric mice were generated, each demonstrating signs of PCa malignancy. (*E*) TRAMP-C2 progression in Lck-cre; Klf2$^{fl/fl}$ mice that received naive KLF2^{+} CD4^{+} T cells. One week after s.c. challenge with TRAMP-C2, CD4^{+}CD25^{-} T cells from Klf2$^{fl/fl}$ animals were transferred into three Lck-cre; Klf2$^{fl/fl}$ mice (experimental, black). The remaining four Lck-cre; Klf2$^{fl/fl}$ mice served as controls (red). Mean tumor volume (±SD) at d52 was 1,737 ± 326 (experimental) versus 311 ± 254 (control), $P = 0.001$, calculated by Student's *t* test. (*F*) Newly generated pTregs were located in the draining lymph node, not the tumor, of PCa-bearing mice. Naive CD4^{+} T cells from CD45.1^{+} mice were transferred into Lck-cre; Klf2$^{fl/fl}$ (CD45.2^{+}) recipients that had established TRAMP-C2 cancer; then, de novo pTreg production (CD45.1^{+}CD45.2^{-}CD4^{+}CD25^{+}Foxp3^{+}) was assessed 1 mo later in the tumor and associated draining lymph node (inguinal). The percentage of pTregs are shown. Data are representative of three mice. (*G*) Schematic to test whether tumor-specific pTregs were sufficient to impair anticancer immunity in Lck-cre; Klf2$^{fl/fl}$ mice. Naive CD4^{+} T cells harvested from OT2; Foxp3^{RFP} mice were transferred into Lck-cre; Klf2$^{fl/fl}$ recipients previously challenged s.c. with B16-OVA melanoma. Newly generated pTregs (mRFP^{+} lymphocytes) were then transferred into a second set of Lck-cre; Klf2$^{fl/fl}$ mice challenged with B16-OVA to assess their impact on tumor progression. (*H*) Tumor growth in Lck-cre; Klf2$^{fl/fl}$ mice following the adoptive transfer of tumor-specific pTregs. Melanoma progression was measured in Lck-cre; Klf2$^{fl/fl}$ animals with cancer (1.5×10^4 B16-OVA) that received 1.5×10^5 tumor-specific mRFP^{+} pTregs (black lines). Tumor progression in positive control (Klf2$^{fl/fl}$, blue lines) and negative control (Lck-cre; Klf2$^{fl/fl}$, red lines) animals was measured at the same time. The dashed line demarcates maximal limit for humane tumor burden. N = 3 Klf2$^{fl/fl}$, 5 Lck-cre; Klf2$^{fl/fl}$, and 4 Lck-cre; Klf2$^{fl/fl}$ mice that received mRFP^{+} cells. There is a statistically significant difference ($P < 0.001$) in growth trajectories between the Lck-cre; Klf2$^{fl/fl}$ (red) and Lck-cre; Klf2$^{fl/fl}$+pTregs (black) groups as determined using a linear mixed effects model with the cube root of tumor volume as the response.

production alone was sufficient to maintain antitumor immunity in mice challenged with melanoma or PCa.

Tumor-Specific pTregs Accumulate in the SLOs of Mice that Develop Malignant Cancer. If conversion of tumor-specific $CD4^+$ T cells into pTregs was responsible for cancer progression leading to malignancy, then a PCa-specific pTreg population should have been present in wild-type mice that was absent in (TRAMP); Lck-cre; $Klf2^{fl/fl}$ animals. Therefore, we initially evaluated immune suppression directed against the neoantigen, SV40, for evidence of a tumor-specific pTreg population. Immunotherapies that improve PCa outcome, such as Sipuleucel-T, are associated with T_H1-like immune responses (42). For that reason, we focused on IFNγ-producing $CD4^+$ T cells as a readout of effector T cell responses. TRAMP littermates were challenged with SV40 peptide+adjuvant; then, IFNγ production was evaluated via ELISpot. SV40 peptide-specific $CD4^+$ T cell responses were significantly reduced in TRAMP mice relative to TRAMP; Lck-cre; $Klf2^{fl/fl}$ littermates (Fig. 3 *A*, *Left*), in keeping with the tumor immune-suppressive nature of TRAMP animals. Interestingly, more T_H1 cells were detected in TRAMP mice relative to non-tumor-bearing Lck-cre; $Klf2^{fl/fl}$ animals, which suggested that tumor-specific effector T cells were present in TRAMP mice prior to peptide challenge but were actively inhibited. To test this possibility under alternate conditions, splenocytes from TRAMP cohorts were cultured for 1 wk with SV40 peptide to reactivate effector T cells that had spontaneously developed in cancer-bearing mice; then, T_H1 effector activity was assessed by ELISpot (Fig. 3 *A*, *Right*). Few T_H1 cells arose from TRAMP-derived splenocytes, in contrast to the robust production of IFNγ-producing $CD4^+$ T cells originating from TRAMP; Lck-cre; $Klf2^{fl/fl}$ animals. T_H1 cells were absent in cultures derived from Lck-cre; $Klf2^{fl/fl}$ mice, demonstrating that culture conditions were sufficient to amplify preexisting effector responses but not to develop newly differentiated $CD4^+$ T cell activity. Of note, cocultured splenocytes harvested from TRAMP and TRAMP; Lck-cre; $Klf2^{fl/fl}$ littermates failed to produce a sizable population of IFNγ-producing $CD4^+$ T cells. The absence of effector cells following coculture was not solely due to a dilution effect, in contrast to the response observed when independently cultured $CD4^+$ T cells were mixed at a 1:1 ratio prior to ELISpot detection. Instead, the result with mixed cultured splenocytes indicated that a suppressive population that recognizes tumor antigen was present in TRAMP animals but was absent in TRAMP; Lck-cre; $Klf2^{fl/fl}$ littermates. An initial screen for suppressive cells indicated that TRAMP mice harbored normal Treg frequencies in SLOs, although few Tregs were isolated from the tumor bed (Fig. 3*B*). This latter phenotype is consistent with PCa being classified as a "cold" tumor. To differentiate between tumor-specific pTregs and unrelated Treg populations, we repeated naive $CD4^+$ T cell ($CD45.1^+$) transfer experiments in Lck-cre; $Klf2^{fl/fl}$ animals ($CD45.2^+$), including recipients with established melanoma. As shown in Fig. 3*C*, a small but consistent pool of tumor-specific pTregs could be observed circulating within SLOs of tumor-bearing animals, in contrast to littermate controls. Reduced pTreg frequencies in mice without tumors indicated that most de novo pTreg differentiation was in response to tumor and not alternate exogenous antigens. Importantly, the highest percentage of newly formed pTregs was found in the tumor-associated draining lymph node, which suggested that this was the primary site of pTreg formation/activity. To further aid in our identification of tumor-specific Tregs, we next used a tetramer-based isolation technique to enrich for lymphocytes that bound SV40 peptides in the context of MHC class-II molecules ($I\text{-}A^b$). $Foxp3^+$ Tregs were identified in the spleen but not the thymus of a 6-wk-old TRAMP mouse (Fig. 3*D*), which indicated that the tetramers were isolating peripheral- but not tTregs. The frequency of Tregs varied between tetramers, possibly reflecting peptide immunodominance. Consistent with tetramers isolating tumor-specific pTregs, minimal frequencies of $Foxp3^+$ Tregs were isolated from the thymus or spleen of TRAMP; Lck-cre; $Klf2^{fl/fl}$ littermates. Since SV40 TAg was initially expressed at 4 wk of age in TRAMP mice, detection of tumor-specific pTregs 2 wk later suggested that these inhibitory lymphocytes contributed to early stages of cancer-based immune suppression. Conversely, analysis of a 28-wk-old TRAMP mouse with malignant PCa (Fig. 3*E*) demonstrated that tumor-specific pTregs accumulated in SLOs with the highest frequency occurring in the draining lymph node. Circulating tumor-specific pTregs were also isolated from chimeric TRAMP; Lck-cre; $Klf2^{fl/fl}$ mice (Fig. 3*F*), consistent with their causal role in establishing PCa-directed immune suppression. From this, we conclude that tumor-specific pTregs are generated early during cancer progression and these inhibitory cells accumulate in SLOs to impair continued generation of antitumor immunity.

Endogenous Antitumor Immunity in the Absence of pTregs. Since tumor-specific pTregs were necessary for cancers to escape immune surveillance, blocking the development of these inhibitory lymphocytes provided us with a unique opportunity to study spontaneous antitumor immunity in a preclinical mouse model. PCa is referred to as a cold cancer (43) due to a lack of TILs (*SI Appendix*, Fig. S3); however, immunohistochemistry of prostate from TRAMP; Lck-cre; $Klf2^{fl/fl}$ mice revealed a localized influx of T cells (Fig. 4*A*). In older mice (e.g., 60 wk of age), $CD4^+$ and $CD8^+$ TIL frequencies could appear exaggerated due to the loss of transformed prostate tissue. Occasionally, we detected the generation of tertiary lymphoid structures (*SI Appendix*, Fig. S4); a formation that has been observed in PCa patients who have experienced spontaneous disease remission (44). The majority of TILs were conventional $CD4^+Foxp3^-$ T cells, although $CD8^+$ T cells were present in the tumors, closely associated with transformed epithelial cells (*SI Appendix*, Fig. S5). In fact, an increased frequency of $CD4^+Foxp3^-$ TILs was universally observed in tumor mouse models that lacked pTregs, and conversely, reintroduction of pTregs in chimeric mice reestablished a cold tumor environment (Fig. 4 *B*–*D*). This latter phenotype excluded the possibility that increased TIL frequencies were due to aberrant KLF2-deficient T cell migration patterns. Impaired/exhausted TILs are commonly observed in tumor beds and this observation forms the basis for immune checkpoint blockade (45). Examination of TILs collected from TRAMP mice (Fig. 4*E*) and control animals transplanted with TRAMP-C2 tumors (Fig. 4*F*) confirmed that these cells expressed surface receptors reflective of T cell exhaustion (46), including PD-1, TIM3, and LAG-3. In contrast, TILs isolated from (TRAMP); Lck-cre; $Klf2^{fl/fl}$ expressed lower surface levels of these molecules, indicating that the tumor microenvironment and associated draining lymph nodes were not promoting T cell exhaustion. Another hallmark of a tumor-suppressive microenvironment is the accumulation of myeloid-derived suppressor cells (MDSC), both in the primary tumor and circulation (47). Murine MDSC are a heterogeneous pool of immature myeloid cells that are primarily composed of granulocytic (gMDSC = $CD11b^+Ly6C^{int}Ly6G^+$) and monocytic (mMDSC = $CD11b^+Ly6C^{hi}Ly6G^-$) populations. Low frequencies of MDSC were observed in the spleens of all mice; however, an increased percentage of splenic gMDSC was detected in TRAMP mice relative to TRAMP; Lck-cre; $Klf2^{fl/fl}$ or control animals. Due to issues with Ly6C staining, we could not exclude the possibility that this gMDSC population also included macrophages. This increase in MDSC was most obvious

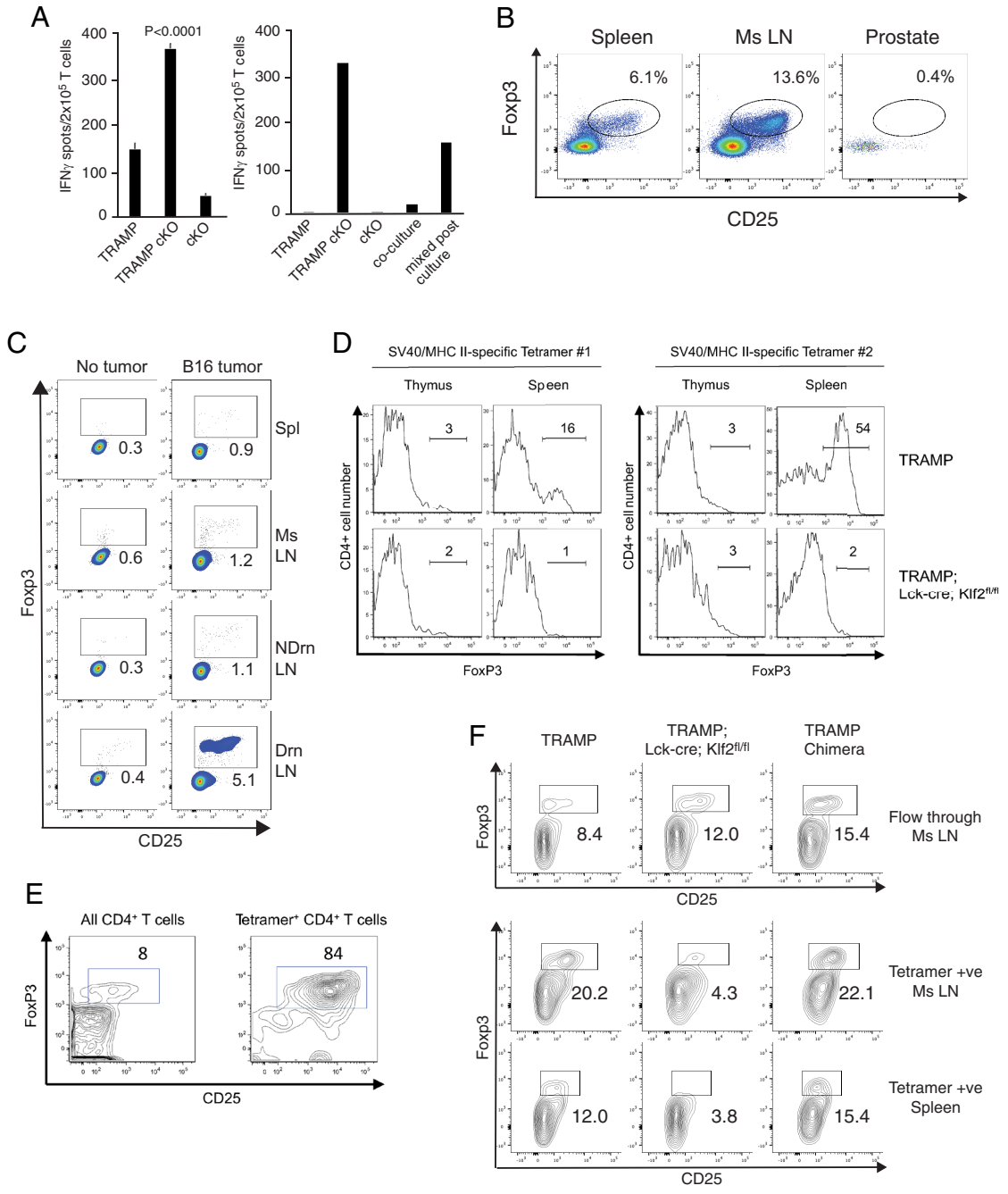

Fig. 3. Tumor-specific pTregs are present in mice that develop malignant PCa but are absent in mice with lasting anti-PCa immunity. (*A*) Tumor-specific $CD4^+$ effector T cell activity was suppressed in mice that harbor pTregs. (*Left*) TRAMP, TRAMP; Lck-cre; $Klf2^{fl/fl}$, and Lck-cre; $Klf2^{fl/fl}$ mice were inoculated with tumor antigen (SV40 peptide)+adjuvant; then, 10 d later, $CD4^+$ T cells were restimulated with a pan-T cell immunogen to quantify IFNγ production via ELISpot. Cells were cultured in triplicate, N = 2 experiments. $P < 0.0001$ for TRAMP versus TRAMP; Lck-cre; $Klf2^{fl/fl}$, as determined by Student's *t* test. (*Right*) Splenocytes from TRAMP, TRAMP; Lck-cre; $Klf2^{fl/fl}$ and $Klf2^{fl/fl}$ mice were individually cultured with SV40 peptide. Additionally, splenocytes from TRAMP and TRAMP; Lck-cre; $Klf2^{fl/fl}$ mice were cocultured with SV40 peptide at a 1:1 ratio. $CD4^+$ T cells were then isolated from cultures and restimulated with a pan-T cell immunogen to quantify IFNγ production by ELISpot. $CD4^+$ T cells isolated from individual TRAMP and TRAMP; Lck-cre; $Klf2^{fl/fl}$ cultures were also mixed at a 1:1 ratio prior to restimulation to demonstrate potential dilution effects. N = 2 experiments. (*B*) Tregs were plentiful in SLOs but scarce in the prostate of TRAMP animals. Treg frequencies ($CD4^+CD25^+Foxp3^+$) in SLOs (spleen, mesenteric lymph nodes) and GU of a 20-wk-old TRAMP mouse. Data are representative of 5 mice, 15 to 20 wk of age. (*C*) De novo generation of pTregs occurred in melanoma-associated draining lymph nodes. Naive $CD4^+(CD25^-)$ T cells from $CD45.1^+$ mice were adoptively transferred into Lck-cre; $Klf2^{fl/fl}$ recipients that had established s.c. B16 melanoma. Lck-cre; $Klf2^{fl/fl}$ mice that received $CD45.1^+$ T cells but lacked tumor served as a control. The percentage of newly generated $CD45.1^+CD90.2^+CD4^+CD25^+Foxp3^+$ Tregs is shown for select tissues, including spleen, mesenteric lymph nodes (Ms LN), inguinal lymph node associated with tumor (Drn LN), and contralateral inguinal lymph node (NDrn LN). N = 3 mice per cohort. (*D*) Tumor-specific pTregs were generated at an early stage of PCa in TRAMP mice. Thymocytes or splenocytes were isolated from 6-wk-old TRAMP and TRAMP; Lck-cre; $Klf2^{fl/fl}$ littermates; then, the cells were passed over a column containing immobilized SV40 peptide/I-A^b tetramer. Two sets of tetramers were used, both of which present an immunogenic sequence of SV40 peptide. T cells that bound to the tetramers were then analyzed by flow cytometry for Foxp3 expression. The % $Foxp3^+CD4^+$ Tregs is shown. N = 3 experiments. (*E*) Tumor-specific pTregs accumulated in the draining lymph node of a 28-wk-old TRAMP mouse. Lymphocytes from the iliac lymph nodes were passed over an SV40 peptide/I-A^b tetramer column and then stained for $CD4^+CD25^+Foxp3^+$ expression. The % Tregs precolumn (*Left* contour plot) and postcolumn (*Right* contour plot) are displayed. N = 2 experiments. (*F*) Identification of tumor-specific pTregs in TRAMP; Lck-cre; $Klf2^{fl/fl}$ chimeric mice. Lymphocytes from TRAMP, TRAMP; Lck-cre; $Klf2^{fl/fl}$, or TRAMP; Lck-cre; $Klf2^{fl/fl}$ chimeric (5:1 ratio of Lck-cre; $Klf2^{fl/fl}$ and $Klf2^{fl/fl}$ bone marrow) age-matched mice were passed over a SV40 peptide/I-A^b tetramer column; then, flow-through (cells that did not bind to the column) and tetramer-bound cells were stained to identify Tregs ($CD4^+CD25^+Foxp3^+$). % Tregs in flow-through (*Top*) and tetramer-positive lymphocytes from mesenteric lymph nodes (*Middle*) or spleen (*Bottom*) are displayed. N = 2 experiments.

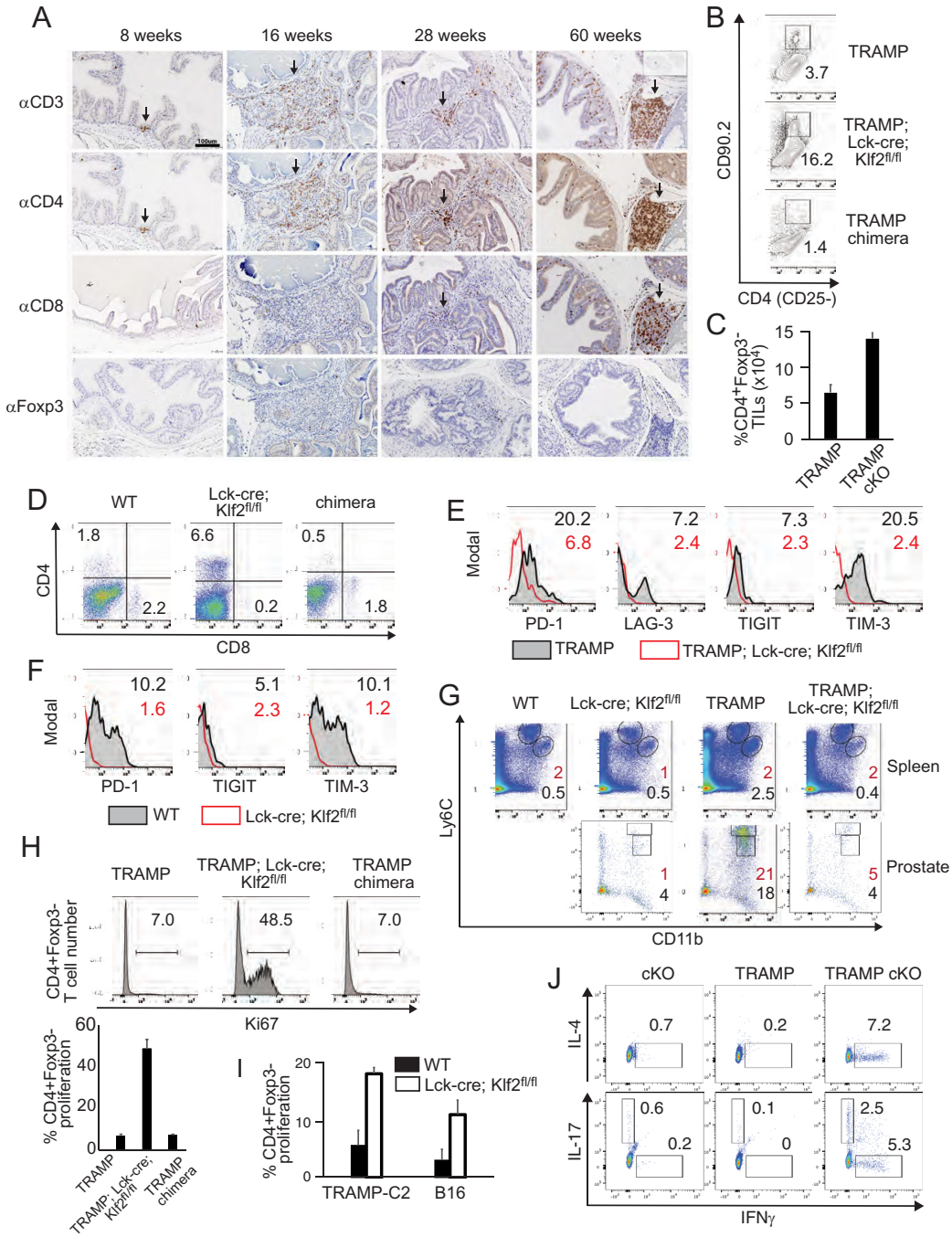

Fig. 4. In the absence of pTregs, spontaneous CD4$^+$ effector T cell activity develops and persists in tumor-bearing animals. (*A*) Immunohistochemistry of prostate from TRAMP; Lck-cre; Klf2$^{fl/fl}$ mice at early (8 wk), intermediate (16 wk), late (28 wk), and very late (60 wk) stages of autochthonous PCa. Serial sections of prostate tissue were stained to identify infiltrating T cells (αCD3), T_H cells (αCD4), CTLs (αCD8), and Tregs (αFoxp3). 20× magnification. Arrows identify sites of lymphocyte infiltration. (*B*) Frequency of tumor-infiltrating CD4$^+$ T cells in 35-wk-old TRAMP, TRAMP; Lck-cre Klf2$^{fl/fl}$, and TRAMP; Lck-cre; Klf2$^{fl/fl}$ mixed bone marrow chimeric mice. Contour plots display % of conventional CD4$^+$ T cells. N = 1 experiment. (*C*) Frequency of CD4$^+$Foxp3$^-$ TILs in 22-wk-old TRAMP and TRAMP; Lck-cre; Klf2$^{fl/fl}$ mice. Five mice per group, $P < 0.0001$ as determined by Student's test. (*D*) Frequency of TILs in mice challenged with TRAMP-C2 for 8 wk. % of CD4$^+$Foxp3$^-$ and CD8$^+$ TILs present in a Klf2$^{fl/fl}$ (WT), Lck-cre; Klf2$^{fl/fl}$, and Lck-cre; Klf2$^{fl/fl}$ mouse reconstituted with a 5:1 ratio of Lck-cre; Klf2$^{fl/fl}$ and Klf2$^{fl/fl}$ bone marrow (chimera) are displayed. Data are representative of three experiments. (*E*) Exhaustion markers on CD4$^+$Foxp3$^-$ TILs harvested from TRAMP (black) versus TRAMP; Lck-cre; Klf2$^{fl/fl}$ (red) mice at 22 wk of age. Histogram overlays of CD4$^+$Foxp3$^-$ T cells as analyzed by flow cytometry. Mean fluorescent intensity (MFI) of KLF2+ (black) and KLF2-deficient cells (red) are shown. N = 3 experiments. (*F*) Exhaustion markers on CD4$^+$Foxp3$^-$ TILs isolated from Klf2$^{fl/fl}$ (black) versus Lck-cre; Klf2$^{fl/fl}$ (red) mice challenged with TRAMP-C2 for 8 wk. MFI of KLF2+ (black) and KLF2-deficient cells (red) are shown. N = 2 experiments. (*G*) Frequency of MDSC found in the spleen (*Top*) and prostate (*Lower*) of Klf2$^{fl/fl}$ (WT), Lck-cre; Klf2$^{fl/fl}$, TRAMP, and TRAMP; Lck-cre; Klf2$^{fl/fl}$ mice at 16 wk of age. The % of mMDSC (CD11b$^+$Ly6C^{hi}, red font) and gMDSC (CD11b$^+$Ly6c^{int}, black font) is shown. N = 2 experiments. (*H*) IL-2 responsive effector T cells circulated in TRAMP; Lck-cre; Klf2$^{fl/fl}$ mice but were absent in mice with pTregs. T cells harvested from a TRAMP, TRAMP; Lck-cre; Klf2$^{fl/fl}$, or TRAMP; Lck-cre; Klf2$^{fl/fl}$ mouse reconstituted with a 5:1 ratio of Lck-cre; Klf2$^{fl/fl}$ and Klf2$^{fl/fl}$ bone marrow (all 16-wk of age) were cultured with IL-2 (100 U/mL, 4 d); then, proliferation was quantified by Ki67 expression. (*Upper*) A representative histogram with % proliferating CD4$^+$Foxp3$^-$ T cells. (*Lower*) Cumulative data from triplicate cultures. Error bars are SD, $P = 0.02$ using a Kruskal–Wallis H test. N = 2 experiments. (*I*) IL-2 responsive effector CD4$^+$ T cells were present in Lck-cre; Klf2$^{fl/fl}$ mice challenged with TRAMP-C2 (*Left* bars) or B16 (*Right* bars) tumor cells. Splenocytes from tumor-bearing Klf2$^{fl/fl}$ (black) and Lck-cre; Klf2$^{fl/fl}$ (white) mice were cultured with IL-2 (100 U/mL, 4 d); then, proliferation was assessed by Ki67 surface expression. Cells were cultured in triplicate, error bars are SD. $P = 0.0014$ for TRAMP-C2 (N = 3 experiments), $P < 0.0001$ for B16 (N = 2 experiments). (*J*) T_H1 and T_H17 effector cells were present in tumor-bearing mice that lack pTregs. T_H1 (IFNγ), T_H2 (IL-4), and T_H17 (IL-17) differentiation was assessed by restimulating lymphocytes harvested from the mesenteric lymph nodes of Klf2$^{fl/fl}$ (cKO), TRAMP, and TRAMP; Lck-cre; Klf2$^{fl/fl}$ (TRAMP cKO) littermates. The percentage of gated lineages is shown. N = 3 mice per cohort.

in the prostate, where significant populations of mMDSC and gMDSC could be observed in TRAMP mice relative to littermates (Fig. 4*G* and *SI Appendix*, Fig. S6). Thus, it appears that tumor-specific pTregs directly or indirectly promoted production of MDSC populations associated with poor clinical outcomes in cancer patients. Conversely, pTregs impaired tumor-specific T cell responses (Figs. 1*A* and 3*A*), TIL recruitment (Fig. 4 *A*–*D*), and effector activity (Fig. 4 *E* and *F*). Effector T cells require IL-2 for survival and Tregs are known to suppress T cell activity by sequestering this cytokine (48–52); therefore, we were interested in determining the status of IL-2-dependent effector T cells in tumor-bearing animals. As shown in Fig. 4*H*, a pool of IL-2 responsive effector T cells was present in the circulation of tumor-bearing mice that lacked pTregs. In contrast, reintroduction of pTregs prevented effector T cell accumulation in SLOs. De novo generation of effector T cells in pTreg-deficient mice was not limited to a specific cancer model, as evidenced by the presence of IL-2 responsive T cells in Lck-cre; $Klf2^{fl/fl}$ mice transplanted with TRAMP-C2 or B16 tumor cells (Fig. 4*I*). Restimulation of circulating T cells harvested from TRAMP; Lck-cre; $Klf2^{fl/fl}$ mice indicated that the $CD4^+$ T cell pool included a population of T_H1 and T_H17 effector cells (Fig. 4*J*). The former lineage correlates with beneficial antitumor responses whereas the latter lineage has been shown to transdifferentiate into T_H1 and pTregs within the context of a tumor microenvironment (53). These populations were absent in Lck-cre; $Klf2^{fl/fl}$ and TRAMP animals, demonstrating that $T_H1/17$ effector activity was both tumor-dependent and inhibited by pTregs. Therefore, we concluded that in the absence of tumor-specific pTregs, anticancer effector T cells were continuously generated and effectively infiltrated cold tumor microenvironments. This included a large population of conventional $CD4^+$ T cells. In contrast, reintroduction of tumor-specific pTregs in SLOs was sufficient to restore cold tumors, limit the generation of effector T_H1 and T_H17 cells, and promote TIL exhaustion.

Discussion

Cancer treatments that target the host immune system have significant advantages over conventional therapies, including a lack of selective pressure for tumor mutation/escape and potential universality of action. Cancers avoid immune clearance by co-opting peripheral tolerance mechanisms and thus understanding the immune-based events contributing to tumor survival is a medical priority. Numerous white blood cell lineages and corresponding effector functions participate in peripheral tolerance; however, data from the present study suggest that the multi-tiered accumulation of suppressive cells occurs in a coordinated manner that starts with the generation of tumor-specific pTregs. Within 2 wk of epithelial transformation, SV40-reactive pTregs were detected in secondary lymph organs of TRAMP animals. Likewise, a rapid conversion of naive $CD4^+$ T cells into pTregs was observed in tumor-bearing mice. As such, detection of tumor-specific pTregs may serve as an early biomarker for cancer screening. Tumor-specific pTregs accumulated in draining lymph nodes, although work with chimeric mice and adoptive $CD4^+$ T cell or pTreg transfer experiments suggested that relatively few pTregs were needed to maintain tolerance toward cancer. Blocking pTreg formation did not inhibit epithelial cell transformation or early stages of PCa. Instead, a lack of pTregs allowed for the continuance of spontaneous adaptive immunity, which was sufficient to prevent malignancy. Importantly, antitumor responses occurred without the onset of autoimmunity or other immune-related adverse events that hinder current immunotherapies (54, 55). These results suggest that Tregs support peripheral tolerance against a discrete set of peptides, some of which are lineage-specific. We posit that tTregs prevent autoimmunity and suppress antitumor immunity directed against self-antigens (*SI Appendix*, Fig. S7). Conversely, pTregs prevent antitumor immunity directed against neoantigens, and thus, elimination of this suppressive lineage reveals a spectrum of proteins that can be targeted by tumor-specific T cells. In the absence of pTregs, host immunity naturally recognizes transformed cells and establishes an adaptive immune response that infiltrates the tumor bed. This includes a significant influx of effector $CD4^+$ T cells that migrate near, but not identical to cytolytic $CD8^+$ T cells. On rare occasions, this influx also includes the generation of tertiary lymphoid structures. Infiltrating lymphocytes do not display "exhaustion" surface markers nor do MDSCs accumulate in the tumor bed, which indicates that pTregs either directly or indirectly contribute to suppressive events associated with poor prognosis in cancer patients.

Although pTregs are important for suppressing TIL recruitment and promoting exhaustion, results suggest that pTreg-mediated inhibition does not occur in the tumor itself but instead in draining lymph nodes. PCa is classified as a cold tumor, and flow cytometry and immunohistochemistry confirmed that few Tregs were present in the tumor bed (Figs. 2*F* and 3*B* and *SI Appendix*, Fig. S4). On the other hand, we detected a relatively abundant population of tumor-specific pTregs in draining lymph nodes (Figs. 2*F* and 3 *C* and *E*). Effector T cells are generated in lymph nodes that are distal to tumors. If pTreg-mediated suppression was tumor centric, then continued production of effector T cells should have been observed in SLOs. Instead, circulating effector T cells were constrained in tumor-bearing mice that generated pTregs (Figs. 4 *H*–*J*), consistent with T cell suppression in lymph nodes. Tumors are heterogenous tissues with a dispersed T cell population, which creates a physically challenging environment for antigen-specific pTreg suppression. Conversely, SLOs are compact, organized structures that coordinate T cell–antigen-presenting cell interactions; optimal conditions for pTreg-mediated suppression of naive T cells. Therefore, eliminating Tregs located in draining lymph nodes associated with tumors may prove to be more clinically advantageous than targeting Tregs in general or even Tregs found in the tumor bed itself.

The current study has demonstrated that blocking pTreg production safely acts as a prophylactic to impair tumor growth. Future studies will determine whether blocking pTreg production is sufficient to treat preclinical animal models with established cancer. If pTregs have a relatively short half-life and other suppressive lineages rely on pTregs for support, then a temporary block in pTreg generation may act as a monotherapy. Alternatively, blocking new pTreg production while simultaneously reestablishing antitumor immunity may improve the efficacy of current immunotherapies, including immune checkpoint inhibitors, T cell transfer therapies, and treatments that temporarily revive antitumor T cell activity such as Sipuleucel-T (an FDA-approved immunotherapy for advanced PCa). Evidence that blocking pTreg activity improves cancer therapies will also serve as an impetus to design new methods to temporarily eliminate this suppressive T cell lineage.

Materials and Methods

Mice. Lck-cre; $Klf2^{fl/fl}$ and Foxp3-cre; $Klf2^{fl/fl}$ mice were generated as described (16). TRAMP (003135), C57BL/6 J (000664), B6 CD45.1(002014), OT2 (004194), and $Foxp3^{RFP}$ (008374) mice were purchased from Jackson Laboratories. Mice were housed in specific pathogen-free conditions in accordance with the Institutional Animal Care and Use Committee at Vanderbilt University and Wayne State University. Male mice were used for PCa studies. To reduce animal numbers, female littermates were used for B16 melanoma studies.

Transplantation of Tumor Cell Lines. B16F0 cells (CRL-6322) and TRAMP-C2 cells (CRL-2731) were purchased from ATCC and maintained for fewer than three passages. TRAMP-C2 cells were cultured in Dulbecco's modified Eagle's medium (DMEM) supplemented with 5 μg/mL bovine insulin, 10 nM dehydroisoandrosterone, 5% fetal bovine serum (FBS), 5% Nu-Serum IV, 100 U/mL penicillin, and 100 μg/mL streptomycin. B16 cells were cultured in DMEM supplemented with 10% FBS and antibiotics. Tumor growth experiments were performed using 8 to 11-wk-old mice that were s.c. inoculated on the right inguinal region. A total of 10^4 B16F0 cells in log-phase growth were injected (50 μL volume) into all mice without Matrigel. A total of 1.5×10^6 TRAMP-C2 cells in log-phase growth were mixed at a 1:1 ratio with high-concentration Matrigel matrix (BD Biosciences) and injected (100 μL volume) into $Klf2^{fl/fl}$ mice. A total of 1.0×10^6 TRAMP-C2 cells suspended in Matrigel were injected into Lck-cre; $Klf2^{fl/fl}$ littermates. A reduced initial tumor load was used for gene-targeted mice to maintain similar growth curves between cohorts for the first 3 wk of the experiment, the time period at which tumor-mediated immune suppression is being established. Tumor growth was monitored by caliper measurement, and tumor volume was calculated as (WxWxL)/2.

Single-Cell Isolation. Single-cell suspensions were made from spleen, lymph nodes, bone marrow, prostate, and s.c. solid tumors for flow cytometric analysis. Splenic erythrocytes were lysed using an ammonium-chloride-potassium lysis buffer (150 mM NH_4Cl, 10 mM $KHCO_3$, and 0.1 mM EDTA). Genitourinary tract (GU, which included prostate, seminal vesicles, and urethra) and solid tumor were minced with a razor blade and digested with collagenase I (4 mg/mL; Gibco) and collagenase IV (10 mg/mL; Gibco) in IMDM (HyClone) for 1 h at 37 °C. All tissues were mechanically dissociated and passed through 70-μm cell strainers. Single-cell suspensions of prostate and tumor tissue were additionally passed over Lympholyte-M density separation medium (Cedarlane) to concentrate white blood cells. Cells were counted using a hemocytometer and trypan blue to exclude dead cells.

Antibody staining. Anti-CD8α (53-6.7), -CD16/32 (2.4G2), -CD25 (PC61), -CD45.1 (A20), -CD223 (LAG-3, C9B7W), -CD279 (PD-1, J43), and -Ki67 were purchased from BD Pharmingen. Anti-CD4 (GK1.5), -CD90.2 (53-2.1), -CD45.2 (104), -CD366 (TIM3), -TIGIT (Vstm3), and CFSE were purchased from BioLegend. Anti-Ly6c (HK1.4), -Ly6g (1A8), and -Foxp3 (Kjk-15 s) were purchased from Invitrogen. Cells were initially cultured with Fc block prior to surface staining at 4 °C for 20 to 30 min, and then, cells were washed twice before analysis. CFSE staining was performed according to the manufacturer's instructions. Foxp3 and Ki67 staining was done in concert with an intranuclear fixation and permeabilization kit (Invitrogen).

Flow Cytometry. Standard flow cytometric techniques were used to acquire data on a 4- and 5-laser LSRII (BD Biosciences), a 3-laser FACSCanto II (BD Biosciences), and a 3-laser CyAn ADP (Beckman Coulter). Analysis was performed using FlowJo (TreeStar) software. For analysis of T cell lineages, cell suspensions were stained using antibodies directed against CD16/32 (unconjugated "Fc block"), CD90.2, CD4, CD8, CD25, and Foxp3. For analysis of MDSC lineages, cell suspensions were stained using antibodies directed against CD16/32, CD45, CD11b, Ly6C, Ly6G, and DAPI (to exclude dead/dying cells).

Histology and Immunohistochemistry. GU or solid tumor was removed from killed animals and then stored in 10% formalin solution in neutral buffer (Sigma) at 4 °C until processing. Tissues were cut into 2 to 3 mm slices and rinsed in water for 45 min. Tissues were then rehydrated at room temperature (RT) for 45 min each with 70% ethanol, 95% ethanol, 100% ethanol, and xylene. Tissues were immersed in paraffin at 58 °C for 45 min using a Sakura Tissue-TekIV Embedding center (Sakura, Mars, PA). Four-micrometer sections were then placed in a 43 °C water bath and collected on coated glass slides (SuperFrost/Plus; Fisher Scientific, Pittsburgh, PA). The slides were dried overnight at RT. Sections were deparaffinized with three washes of xylene (5 min per wash) followed by three washes of 100% ethanol (2 min per wash). Next, slides were transferred to 95% ethanol, 70% ethanol, and then water for 3 min each. Following this, an antigen retrieval procedure was performed with a Decloaking Chamber (Biocare Medical, Concord, CA) with citrate buffer (10 mM sodium citrate, pH6) for 45 min at a constant temperature of 125 °C (15 p.s.i). Slides were washed in EnVision FLEX wash buffer (Dako, Carpinteria, CA) for 2 min followed by blocking with 10% goat serum in phosphate buffered saline (PBS) (pH7.4) for 10 min. Antibodies were diluted in 0.5% bovine serum albumin in PBS (pH7.4) and incubated with the tissue sections for 1 h at RT. Primary antibodies included CD3 (Dako, rabbit polyclonal), CD4 (BD Biosciences, clone RM4-5), CD8 (BioLegend, clone 53-6.7), Foxp3 (eBioscience, clone FJK-16S), B220 (BD Biosciences, clone RA3-6B2), and SV40 TAg (BD Pharmingen, clone PAb 108). The slides were then rinsed twice for 10 min with EnVision FLEX wash buffer. Immunohistochemical reactions were performed using a VECTASTAIN Elite ABC kit (PK-6100; Vector Laboratories, Burlingame, CA) with biotinylated anti-rabbit (1:1,000 dilution) or anti-rat IgG (1:500 dilution) (BA-9400 and BA-9401, respectively; Vector Laboratories) for 1 h. The sections were then washed twice with PBS (2 min each) followed by incubation with VECTASTAIN Elite ABC reagent for 30 min. After the slides were washed twice with PBS, the samples were incubated in freshly prepared 0.1% 3,3′-diaminobenzidine solution (Dako) for less than 5 min. The sections were rinsed in water for 2 min, counterstained with Mayer's hematoxylin for 30 s, and then rinsed in water for 2 min. The slides were treated with 70% and 95% ethanol and then three changes of 100% ethanol and xylene (2 min each) prior to mounting with Clear Mount (American MasterTech Scientific, Lodi, CA). Slides were scanned on an Aperio AT2 ScanScope (Leica Biosystems, Buffalo Grove, IL), and digital images were viewed using the ImageScope application (Leica Biosystems). Digital images were captured and processed using Photoshop software (Adobe Systems, San Jose, CA).

Generation of Mixed Bone Marrow Chimeric Animals. Eight-week-old recipient mice were irradiated twice (550 rad/dose), separated by 3 h, using an X-RAD 320 Irradiator. After 24 h, T cell–depleted bone marrow cells (10^7 cells) were transferred via intraorbital injection into recipient mice (TRAMP; Lck-cre; $Klf2^{fl/fl}$ for TRAMP studies, Lck-cre; $Klf2^{fl/fl}$ mice for TRAMP-C2 studies). Bone marrow was harvested from $KI2^{fl/fl}$ and Lck-cre; $Klf2^{fl/fl}$ mice (8 to 12 wk) and mixed at a 1:5 ratio in sterile PBS prior to adoptive transfer. Recipient mice were placed on a sulfamethoxazole and trimethoprim oral solution (Pharmaceutical Associates, Inc.) for 3 wk to prevent opportunistic infection. For TRAMP-C2 studies, chimeric mice were rested 8 wk prior to s.c. challenge with tumor cells to ensure full reconstitution of the adaptive immune system.

TRAMP-C2 Tumor Growth in Lck-cre; $Klf2^{fl/fl}$ Mice ± Naive $CD4^+$ T Cells. Naive $CD4^+CD25^-$ splenic T cells were isolated from $Klf2^{fl/fl}$ mice using a Mouse Naïve $CD4^+$ T Cell Isolation Kit (12210–150, Akadeum Life Sciences). A total of 5×10^6 naive $CD4^+$ T cells were transferred i.p. into Lck-cre; $Klf2^{fl/fl}$ mice 1 wk after recipient mice had been s.c. transplanted with 1×10^6 TRAMP-C2 tumor cells. To account for potential turnover of adoptively transferred cells, a further 5×10^6 naive $CD4^+$ T cells were injected i.p. 3 wk later.

Assessment of Tumor-Associated pTreg Production. Lck-cre; $Klf2^{fl/fl}$ mice were challenged s.c. with 1×10^6 TRAMP-C2 tumor cells (males) or 1×10^4 B16 melanoma cells (females). Two weeks later, mice received 5×10^6 naive $CD4^+$ T cells isolated (Naïve $CD4^+$ T cell isolation kit, Miltenyi Biotec) from $CD45.1^+$ donors of their respective sex. An additional cohort of Lck-cre; $Klf2^{fl/fl}$ mice that did not have cancer also received $CD45.1^+$ T cells to control for tumor-mediated pTreg generation. Tissues from cancer-bearing mice were harvested and examined at humane end points; controls were examined at the same time.

Adoptive Transfer of Tumor-Specific pTregs. Female Lck-cre; $Klf2^{fl/fl}$ mice were injected s.c. with B16-OVA melanoma (1.5×10^4 cells, ATCC). Two weeks later, the same animals received 5×10^6 naive $CD4^+$ T cells harvested from female OT2; $Foxp3^{RFP}$ mice using a Miltenyi Biotec Naïve $CD4^+$ T cell isolation kit. After 10 d, red fluorescent T cells harvested from the spleens of recipient animals were isolated using a Sony Biotechnology SY3200 Sorter (sorted purity was >99% $CD4^+Foxp3^+$). The $mRFP^+$ T cells (1.5×10^5 cells/recipient) were transferred into female Lck-cre; $Klf2^{fl/fl}$ mice that had been injected s.c. with B16-OVA melanoma (1.5×10^4) 10 d prior to adoptive transfer. Two littermate cohorts ($Klf2^{fl/fl}$ and Lck-cre; $Klf2^{fl/fl}$) were similarly challenged with B16-OVA; however, these animals did not receive $mRFP^+$ cells. Tumor progression was measured until humane end points were met ($Klf2^{fl/fl}$ and Lck-cre; $Klf2^{fl/fl}$ mice with $mRFP^+$ cells) or the experiment was terminated (Lck-cre; $Klf2^{fl/fl}$ controls).

Measurement of $CD4^+$ T Cell IFNγ Production. Twelve-week-old TRAMP, TRAMP; Lck-cre; $Klf2^{fl/fl}$, and $Klf2^{fl/fl}$ littermates were inoculated s.c. with 100 μL SV40 TAg 529–543 peptide (50 μg) suspended 1:1 with Complete Freund's Adjuvant (Sigma-Aldrich). Ten days later, splenic $CD4^+$ T cells were isolated using a negative-selection Mouse $CD4^+$ T Cell Isolation kit (12210–130, Akadeum Life Sciences) according to the manufacturer's instructions. Alternatively, splenocytes

(2 to 5 × 10^6 cells/mL) from uninoculated 12-wk-old TRAMP, TRAMP; Lck-cre; Klf2$^{fl/fl}$, and Lck-cre; Klf2$^{fl/fl}$ littermates were cultured with SV40 TAg 529 to 543 peptide (10^{-6}M) in media (Iscove's Modified Dulbecco's Medium supplemented with 10% fetal calf serum, glutamine, antibiotics, and 5 μm β-mercaptoethanol) for 7 d in a humidified 5% CO_2 incubator. CD4$^+$ T cells were then isolated using a Mouse CD4$^+$ T Cell Isolation kit (12210-130, Akadeum Life Sciences). In both cases, purified CD4$^+$ T cells were analyzed for IFNγ production using a Mouse IFNγ ELISpot^{PLUS} Kit (Mabtech Inc.). Effector CD4$^+$ T cells were restimulated [Ultra-LEAF purified anti-mouse CD3ε (145-2C11, BioLegend) and CD28 (37.51, BioLegend)] and placed in 96-well plates that were precoated with IFNγ mAb (AN18). Two days later, the cells were discarded, and the plates were washed with PBS. Spots associated with secreted IFNγ were detected according to kit instructions (Mabtech Inc.). The plates were then read using an ELISPOT reader (Immunospot, Cellular Technology Ltd.).

Tetramer-Based T Cell Isolation. The MHC class II (I-A^b) tetramers SV40 TAg 529–543 (NEYSVPKTQARFVK, PE-conjugated), SV40 TAg 526–540 (VTMNEYSVPKTQAR, APC-conjugated), and control (PVSKMRMATPLLMQA, both PE- and APC-conjugated) were obtained from the NIH Tetramer Core Facility at Emory University. Single-cell suspensions (5 × 10^6 cells/mL) were Fc blocked for 15 min, and then, the cells were incubated with 10 nM tetramers at RT for 1 h. After washing the cells to remove unbound tetramer, the cells were incubated with anti-PE or anti-APC microbeads (Miltenyi Biotec) for 30 min at 4 °C. The cells were washed to remove excess beads, and then, the cell suspension was passed over an LD column (Miltenyi Biotec) according to instructions. Tetramer-bound cells were then stained (anti-CD4, -CD8, -CD25, -CD90.2, and -Foxp3) using standard techniques and analyzed via flow cytometry.

IL-2 Response Assays. Erythrocyte-depleted splenocytes (5 to 10 × 10^6 cells/mL) were cultured in media (IMDM, 10% fetal calf serum (FCS), nonessential amino acids, antibiotics, 5 μm β-mercaptoethanol) supplemented with IL-2 (100 U/mL, BioLegend) for 96 h. Additional IL-2 (100 U/mL) was added at 48 h. Cell proliferation was measured by staining for surface expression of Ki67 via flow cytometry. Alternatively, precultured cells were stained with CFSE (ThermoFisher Scientific) per the manufacturer's instructions; then, proliferation was assessed as % of cells that diluted expression of the membrane-incorporated dye.

Intracellular Staining for T_H Cell Differentiation. Staining for T_H differentiation was performed using a Mouse $T_H1/T_H2/T_H17$ Phenotyping Kit (BD Pharmingen). Briefly, splenocytes harvested from TRAMP versus TRAMP; Lck-cre; Klf2$^{fl/fl}$ versus Klf2$^{fl/fl}$ littermates were depleted of red blood cells, Fc blocked, and then stained for the pan-T cell marker, CD90.2. The cells (10^7 cells/mL) were then stimulated with PMA (50 ng/mL) and ionomycin (1 μg/mL) in the presence of BD GolgiStop for 6 h at 37 °C. The cells were then fixed, permeabilized, and stained with a cocktail of antibodies directed against CD4, IFNγ, IL-4, and IL-17A.

Data, Materials, and Software Availability. All study data are included in the article and/or *SI Appendix*.

ACKNOWLEDGMENTS. We thank Robert Matusik, Wei-Zen Wei, and Kay-we Wagner for insightful comments and advice, the Wayne State University Microscopy, Imaging and Cytometric Resources Core for assistance, and the NIH Tetramer Core Facility at Emory University for the provision of MHC class-II restricted tetramers. This study was supported by NIH NCI T32 grant CA009531 (J.H.), the Elsa U. Pardee Foundation (HG), the Center for Genomic Pathology at UC Davis (A.D.B.), NCI U01CA196406 (A.D.B.), DOD PCRP grant PC140122 (L.V.K. and E.S.), NCI P30-CA022453 (G.D. and E.S.), and American Cancer Society grant DBG-23-103670-01-IBCD (E.S.). The Microscopy, Imaging and Cytometric Resources Core is supported by NIH Center grants P30 CA22453 and R50 CA251068-01.

Author affiliations: [a]Department of Biochemistry, Microbiology and Immunology, Wayne State University Medical School, Detroit, MI 48201; [b]Department of Oncology, Wayne State University Medical School, Detroit, MI 48201; [c]Department of Pathology, Microbiology and Immunology, Vanderbilt University Medical Center, Nashville, TN 37232; [d]Tumor Biology and Microenvironment Research Program, Barbara Ann Karmanos Cancer Institute, Detroit, MI 48201; and [e]Department of Pathology and Laboratory Medicine, Center for Comparative Medicine, University of California Davis, Davis, CA 95616

1. R. Khattri, T. Cox, S. A. Yasayko, F. Ramsdell, An essential role for scurfin in Cd4+Cd25+ T regulatory cells. *Nat. Immunol.* **4**, 337–342 (2003).
2. J. D. Fontenot, M. A. Gavin, A. Y. Rudensky, Foxp3 programs the development and function of Cd4+Cd25+ regulatory T cells. *Nat. Immunol.* **4**, 330–336 (2003).
3. R. S. Wildin *et al.*, X-Linked neonatal diabetes mellitus, enteropathy and endocrinopathy syndrome is the human equivalent of mouse scurfy. *Nat. Genet.* **27**, 18–20 (2001).
4. J. Shimizu, S. Yamazaki, S. Sakaguchi, Induction of tumor immunity by removing Cd25+Cd4+ T cells: A common basis between tumor immunity and autoimmunity. *J. Immunol.* **163**, 5211–5218 (1999).
5. J. Dannull *et al.*, Enhancement of vaccine-mediated antitumor immunity in cancer patients after depletion of regulatory T cells. *J. Clin. Invest.* **115**, 3623–3633 (2005).
6. S. A. Fisher *et al.*, Transient Treg depletion enhances therapeutic anti-cancer vaccination. *Immun. Inflamm. Dis.* **5**, 16–28 (2017).
7. K. Klages *et al.*, Selective depletion of Foxp3+ regulatory T cells improves effective therapeutic vaccination against established melanoma. *Cancer Res.* **70**, 7788–7799 (2010).
8. E. N. Klyushnenkova *et al.*, Breaking immune tolerance by targeting Cd25+ regulatory T cells is essential for the anti-tumor effect of the Ctla-4 blockade in an Hla-Dr transgenic mouse model of prostate cancer. *Prostate* **74**, 1423–1432 (2014).
9. M. W. Teng *et al.*, Conditional regulatory T-cell depletion releases adaptive immunity preventing carcinogenesis and suppressing established tumor growth. *Cancer Res.* **70**, 7800–7809 (2010).
10. S. Z. Josefowicz, L. F. Lu, A. Y. Rudensky, Regulatory T cells: Mechanisms of differentiation and function. *Ann. Rev. Immunol.* **30**, 531–564 (2012).
11. A. M. Bilate, J. J. Lafaille, Induced Cd4+Foxp3+ regulatory T cells in immune tolerance. *Ann. Rev. Immunol.* **30**, 733–758 (2012).
12. A. K. Abbas *et al.*, Regulatory T cells: Recommendations to simplify the nomenclature. *Nat. Immunol.* **14**, 307–308 (2013).
13. S. Hori, M. Haury, A. Coutinho, J. Demengeot, Specificity requirements for selection and effector functions of Cd25+4+ regulatory T cells in anti-myelin basic protein T cell receptor transgenic mice. *Proc. Natl. Acad. Sci. U.S.A.* **99**, 8213–8218 (2002).
14. Q. Tang *et al.*, In vitro-expanded antigen-specific regulatory T cells suppress autoimmune diabetes. *J. Exp. Med.* **199**, 1455–1465 (2004).
15. D. R. Tonkin, J. He, G. Barbour, K. Haskins, Regulatory T cells prevent transfer of type 1 diabetes in nod mice only when their antigen is present in vivo. *J. Immunol.* **181**, 4516–4522 (2008).
16. P. G. Coulie, B. J. Van Den Eynde, P. Van Der Bruggen, T. Boon, Tumour antigens recognized by T lymphocytes: At the core of cancer immunotherapy. *Nat. Rev. Cancer* **14**, 135–146 (2014).
17. S. K. Pabbisetty *et al.*, Klf2 is a rate-limiting transcription factor that can be targeted to enhance regulatory T-cell production. *Proc. Natl. Acad. Sci. U.S.A.* **111**, 9579–9584 (2014).
18. L. Granziero *et al.*, Adoptive immunotherapy prevents prostate cancer in a transgenic animal model. *Eur. J. Immunol.* **29**, 1127–1138 (1999).
19. A. A. Hurwitz *et al.*, Combination immunotherapy of primary prostate cancer in a transgenic mouse model using Ctla-4 blockade. *Cancer Res.* **60**, 2444–2448 (2000).
20. M. Fasso *et al.*, Spas-1 (Stimulator of prostatic adenocarcinoma-specific T cells)/Sh3glb2: A prostate tumor antigen identified by Ctla-4 blockade. *Proc. Natl. Acad. Sci. U.S.A.* **105**, 3509–3514 (2008).
21. A. R. Elia *et al.*, Targeting tumor vasculature with Tnf leads effector T cells to the tumor and enhances therapeutic efficacy of immune checkpoint blockers in combination with adoptive cell therapy. *Clin. Cancer Res.* **24**, 2171–2181 (2018).
22. S. Wada *et al.*, Sequencing Ctla-4 blockade with cell-based immunotherapy for prostate cancer. *J. Transl. Med.* **11**, 89 (2013).
23. J. R. Gingrich *et al.*, Metastatic prostate cancer in a transgenic mouse. *Cancer Res.* **56**, 4096–4102 (1996).
24. A. Gray *et al.*, Prostate cancer immunotherapy yields superior long-term survival in tramp mice when administered at an early stage of carcinogenesis prior to the establishment of tumor-associated immunosuppression at later stages. *Vaccine* **27**, G52–G59 (2009).
25. Y. Zheng *et al.*, Role of conserved non-coding Dna elements in the Foxp3 gene in regulatory T-cell fate. *Nature* **463**, 808–812 (2010).
26. S. Z. Josefowicz *et al.*, Extrathymically generated regulatory T cells control mucosal Th2 inflammation. *Nature* **482**, 395–399 (2012).
27. K. Nutsch *et al.*, Rapid and efficient generation of regulatory T cells to commensal antigens in the periphery. *Cell Rep.* **17**, 206–220 (2016).
28. C. Schuster, F. Jonas, F. Zhao, S. Kissler, Peripherally induced regulatory T cells contribute to the control of autoimmune diabetes in the nod mouse model. *Eur. J. Immunol.* **48**, 1211–1216 (2018).
29. S. K. Pabbisetty *et al.*, Peripheral tolerance can be modified by altering Klf2-regulated Treg migration. *Proc. Natl. Acad. Sci. U.S.A.* **113**, E4662–E4670 (2016).
30. R. R. Caspi, Immunotherapy of autoimmunity and cancer: The penalty for success. *Nat. Rev. Immunol.* **8**, 970–976 (2008).
31. E. Sebzda, Z. Zou, J. S. Lee, T. Wang, M. L. Kahn, Transcription factor Klf2 regulates the migration of naive T cells by restricting chemokine receptor expression patterns. *Nat. Immunol.* **9**, 292–300 (2008).
32. J. Y. Lee *et al.*, The transcription factor Klf2 restrains Cd4(+) T follicular helper cell differentiation. *Immunity* **42**, 252–264 (2015).
33. J. P. Weber *et al.*, Icos maintains the T follicular helper cell phenotype by down-regulating kruppel-like factor 2. *J. Exp. Med.* **212**, 217–233 (2015).
34. C. Gu-Trantien *et al.*, Cd4(+) follicular helper T cell infiltration predicts breast cancer survival. *J. Clin. Invest.* **123**, 2873–2892 (2013).
35. J. Niogret *et al.*, Follicular helper-T cells restore Cd8(+)-Dependent antitumor immunity and anti-Pd-L1/Pd-1 efficacy. *J. Immunother. Cancer* **9**, e002157 (2021).
36. A. E. Overacre-Delgoffe *et al.*, Microbiota-specific T follicular helper cells drive tertiary lymphoid structures and anti-tumor immunity against colorectal cancer. *Immunity* **54**, 2812–2824.e4 (2021).
37. W. Shi *et al.*, Follicular helper T cells promote the effector functions Of Cd8(+) T cells via the provision of Il-21, which is downregulated due to Pd-1/Pd-L1-mediated suppression in colorectal cancer. *Exp. Cell Res.* **372**, 35–42 (2018).
38. J. Baba *et al.*, Depletion of radio-resistant regulatory T cells enhances antitumor immunity during recovery from lymphopenia. *Blood* **120**, 2417–2427 (2012).

39. Y. Qu *et al.*, Gamma-ray resistance of regulatory Cd4+Cd25+Foxp3+ T cells in mice. *Radiat. Res.* **173**, 148–157 (2010).
40. N. Komatsu, S. Hori, Full restoration of peripheral Foxp3+ regulatory T cell pool by radioresistant host cells in scurfy bone marrow chimeras. *Proc. Natl. Acad. Sci. U.S.A.* **104**, 8959–8964 (2007).
41. B. A. Foster, J. R. Gingrich, E. D. Kwon, C. Madias, N. M. Greenberg, Characterization of prostatic epithelial cell lines derived from transgenic adenocarcinoma of the mouse prostate (Tramp) model. *Cancer Res.* **57**, 3325–3330 (1997).
42. K. Hagihara *et al.*, Neoadjuvant sipuleucel-T induces both Th1 activation and immune regulation in localized prostate cancer. *Oncoimmunology* **8**, e1486953 (2019).
43. M. Bilusic, R. A. Madan, J. L. Gulley, Immunotherapy of prostate cancer: Facts and hopes. *Clin. Cancer Res.* **23**, 6764–6770 (2017).
44. M. L. Garcia-Hernandez *et al.*, A unique cellular and molecular microenvironment is present in tertiary lymphoid organs of patients with spontaneous prostate cancer regression. *Front. Immunol.* **8**, 563 (2017).
45. K. E. Pauken, E. J. Wherry, Overcoming T cell exhaustion in infection and cancer. *Trends Immunol.* **36**, 265–276 (2015).
46. A. M. Miggelbrink *et al.*, Cd4 T-cell exhaustion: Does it exist and what are its roles in cancer? *Clin. Cancer Res.* **27**, 5742–5752 (2021).
47. F. Veglia, E. Sanseviero, D. I. Gabrilovich, Myeloid-derived suppressor cells in the era of increasing myeloid cell diversity. *Nat. Rev. Immunol.* **21**, 485–498 (2021).
48. P. Pandiyan, L. Zheng, S. Ishihara, J. Reed, M. J. Lenardo, Cd4+Cd25+Foxp3+ regulatory T cells induce cytokine deprivation-mediated apoptosis of effector Cd4+ T cells. *Nat. Immunol.* **8**, 1353–1362 (2007).
49. A. M. Thornton, E. E. Donovan, C. A. Piccirillo, E. M. Shevach, Cutting edge: Il-2 is critically required for the in vitro activation of Cd4+Cd25+ T cell suppressor function. *J. Immunol.* **172**, 6519–6523 (2004).
50. D. Busse *et al.*, Competing feedback loops shape Il-2 signaling between helper and regulatory T lymphocytes in cellular microenvironments. *Proc. Natl. Acad. Sci. U.S.A.* **107**, 3058–3063 (2010).
51. T. Yamaguchi *et al.*, Construction of self-recognizing regulatory T cells from conventional T cells by controlling Ctla-4 And Il-2 expression. *Proc. Natl. Acad. Sci. U.S.A.* **110**, E2116–E2125 (2013).
52. T. Chinen *et al.*, An essential role for the Il-2 receptor in T(Reg) cell function. *Nat. Immunol.* **17**, 1322–1333 (2016).
53. S. Downs-Canner *et al.*, Suppressive Il-17a(+)Foxp3(+) And Ex-Th17 Il-17a(Neg)Foxp3(+) T(Reg) cells are a source of tumour-associated T(Reg) cells. *Nat. Commun.* **8**, 14649 (2017).
54. G. Morad, B. A. Helmink, P. Sharma, J. A. Wargo, Hallmarks of response, resistance, and toxicity to immune checkpoint blockade. *Cell* **184**, 5309–5337 (2021).
55. S. Bagchi, R. Yuan, E. G. Engleman, Immune checkpoint inhibitors for the treatment of cancer: Clinical impact and mechanisms of response and resistance. *Annu. Rev. Pathol.* **16**, 223–249 (2021).